Publication Year	2015
Acceptance in OA	2020-03-09T17:32:21Z
Title	High-energy cosmic neutrinos from spine-sheath BL Lac jets
Authors	TAVECCHIO, Fabrizio, GHISELLINI, Gabriele
Publisher's version (DOI)	10.1093/mnras/stv1023
Handle	http://hdl.handle.net/20.500.12386/23185
Journal	MONTHLY NOTICES OF THE ROYAL ASTRONOMICAL SOCIETY
Volume	451

Monthly Notices
of the
ROYAL ASTRONOMICAL SOCIETY

MNRAS **451,** 1502–1510 (2015) doi:10.1093/mnras/stv1023

High-energy cosmic neutrinos from spine-sheath BL Lac jets

F. Tavecchio[★] and G. Ghisellini

INAF – Osservatorio Astronomico di Brera, via E. Bianchi 46, I-23807 Merate, Italy

Accepted 2015 May 5. Received 2015 May 5; in original form 2014 November 11

ABSTRACT

We recently proposed that structured (spine-sheath) jets associated with BL Lac objects could offer a suitable environment for the production of the extragalactic high-energy ($E > 100$ TeV) neutrino recently revealed by IceCube. Our previous analysis was limited to low-power BL Lac objects. We extend our preliminary study to the entire BL Lac population, assuming that the entire diffuse emission is accounted for by these sources. The neutrino output from a single source depends on a relatively large number of parameters. However, for several of them we have constraints coming from observations and previous application of the structured jet model to blazar and radiogalaxy emission. The observed neutrino spectrum then fixes the remaining free parameters. We assume that the power of cosmic rays as well as the radiative luminosity of the sheath depends linearly on the jet power. In turn, we assume that the latter is well traced by the γ-ray luminosity. We exploit the BL Lac γ-ray luminosity function and its cosmic evolution as recently inferred from *Fermi*-LAT data to derive the expected neutrino cumulative intensity from the entire BL Lac population. When considering only the low-power BL Lacs, a large cosmic ray power for each source is required to account for the neutrino flux. Instead, if BL Lacs of all powers produce neutrinos, the power demand decreases, and the required cosmic ray power becomes of the same order of the radiative jet power. In our scheme, the maximum energy of cosmic rays is constrained to be $\lesssim$ few PeV by the lack of events above few PeV. Although such a value is obtained through a fine-tuning with the data, we show that it could be possibly related to the equilibrium between cooling and acceleration processes for high-energy cosmic rays. We also discuss the prospects for the direct association of IceCube events with BL Lacs, providing an estimate of the expected counts for the most promising sources.

Key words: astroparticle physics – neutrinos – radiation mechanisms: non-thermal – BL Lacertae objects: general – gamma-rays: galaxies.

1 INTRODUCTION

The detection of high-energy neutrinos by the IceCube observatory at the South Pole (Aartsen et al. 2013a, 2014) opened a new window for the study of the energetic astrophysical phenomena. The discovery has triggered a wealth of studies devoted to the identification of the possible sources (e.g. Anchordoqui et al. 2014; Murase 2014, for recent reviews). The data are consistent with a flavour ratio $\nu_e : \nu_\mu : \nu_\tau = 1 : 1 : 1$ and the flux level is close to the so-called Waxman–Bahcall limit (Waxman & Bahcall 1999), valid if neutrinos are produced by ultra-high-energy cosmic rays (UHECR; $E > 10^{19}$ eV) through pion-producing hadronic interaction before leaving their – optically thin – sources. However, the energies of the neutrinos ($E_\nu <$ few PeV) indicate that they are associated with cosmic rays (CR) with energies much below the UHECR regime, $E \lesssim 10^{17}$ eV. The substantial isotropy of the flux (with only a non-significant small excess in the direction of the galactic centre) is consistent with an extragalactic origin, although a sizeable contribution from galactic sources cannot be ruled out (e.g. Ahlers & Murase 2014). Possible extragalactic astrophysical sources include propagating CR (e.g. Essey et al. 2010; Kalashev, Kusenko & Essey 2013), star-forming and starburst galaxies (e.g. Loeb & Waxman 2006; Murase, Ahlers & Lacki 2013; Tamborra, Ando & Murase 2014; Wang, Zhao & Li 2014), galaxy clusters (e.g. Murase & Beacom 2013; Zandanel et al. 2014), γ-ray burst (e.g. Waxman & Bahcall 1997; Laha et al. 2013; Petropoulou, Giannios & Dimitrakoudis 2014) and active galactic nuclei (AGN; e.g. Mannheim 1995; Atoyan & Dermer 2003; Kalashev, Semikoz & Tkachev 2015; Kimura, Murase & Toma 2014).

Among AGN, blazars, characterized by the presence of a relativistic jet of plasma moving towards the observer (e.g. Urry & Padovani 1995), have been widely discussed in the past as candidate CR accelerators (e.g. Biermann & Strittmatter 1987; see Kotera

---

[★] E-mail: fabrizio.tavecchio@brera.inaf.it

Published by Oxford University Press on behalf of the Royal Astronomical Society

& Olinto 2011 for a review) and thus potential neutrino emitters (e.g. Atoyan & Dermer 2003; Becker 2008). Murase, Inoue & Dermer (2014) and Dermer, Murase & Inoue (2014) revisited the possibility – already discussed in the past, e.g. Atoyan & Dermer (2003) – that the observed neutrinos are produced in the jet of blazars through photopion reactions involving high-energy CR and soft photons ($p + \gamma \to X + \pi$), followed by the prompt charged pion decay ($\pi^{\pm} \to \mu^{\pm} + \nu_{\mu} \to e^{\pm} + 2\nu_{\mu} + \nu_{e}$; hereafter we do not distinguish among ν and $\bar{\nu}$). Their analysis – based on the simplest, one-zone, framework – led to the conclusion that both the flux level and the spectral shape inferred by the IceCube data are difficult to reproduce by this scenario. In particular they predicted a rapid decline of the emission below 1 PeV. In their framework – in which the CR luminosity is assumed to be proportional to the electromagnetic output – it is naturally expected that the neutrino cumulative flux is dominated by the most luminous and powerful blazars, i.e. the flat-spectrum radio quasars (FSRQ), which are also the sources characterized by the most rich radiative environment (required to have efficient photomeson reactions). BL Lac objects, the low-power blazars defined as those which display faint or even absent optical broad emission lines, would provide only a minor contribution.

As noted, the Murase et al. (2014) analysis relies on the simplest scenario for blazars, assuming that their jets are characterized by a well-localized emission region (hence the definition of one-zone models) with a well-defined speed. In a previous paper (Tavecchio, Ghisellini & Guetta 2014, hereafter Paper I), we reconsidered this issue showing that, under the assumption that the jet presents a velocity structure, i.e. the flow is composed by a fast spine surrounded by a slower sheath (or layer), the neutrino output from the weak BL Lac objects (the so-called highly peaked BL Lacs, HBL) is boosted and could match the observations. The proposal for the existence of a velocity structure of the jet has been advanced as a possible solution for the so-called Doppler crisis for TeV BL Lacs (e.g. Georganopoulos & Kazanas 2003; Ghisellini, Tavecchio & Chiaberge 2005) and to unify the BL Lacs and radiogalaxy populations (e.g. Chiaberge et al. 2000; Meyer et al. 2011; Sbarrato, Padovani & Ghisellini 2014). Direct radio very long baseline interferometry (VLBI) imaging of both radiogalaxies (e.g. Müller et al. 2014; Nagai et al. 2014) and BL Lac (e.g. Giroletti et al. 2004; Piner & Edwards 2014) jets, often showing a 'limb brightening' transverse structure, provides a convincing observational support to this idea, also corroborated by numerical simulations (e.g. McKinney 2006; Rossi et al. 2008). The reason behind the possibility to increase the neutrino (and inverse Compton γ-ray) production efficiency in such a spine-layer structure stems from the fact that for particles flowing in the spine the radiation field produced in the layer appears to be amplified because of the relative motion between the two structures (e.g. Tavecchio & Ghisellini 2008). In this condition, the density of the soft photons in the spine rest frame – determining the proton cooling rate and hence the neutrino luminosity – can easily exceed that of the locally produced synchrotron ones, the only component taken in consideration in the one-zone modelling of Murase et al. (2014) in the case of BL Lacs (for FSRQ, instead, the photon field is thought to be dominated by the radiation coming from the external environment).

In Paper I, we considered only the weakest BL Lac sources – similar to the prototypical TeV blazar Mrk 421 – for which the arguments supporting the existence of the jet structure are the most compelling. Interestingly, a hint of an actual spatial association between the IceCube events and some low-power TeV emitting BL Lac (among which the aforementioned Mrk 421) has been found by Padovani & Resconi (2014). The implied flux is consistent with the upper limits derived by the sophisticated analysis of the IceCube collaboration (Aartsen et al. 2013b, 2014).

There are hints suggesting that a velocity structure could be a universal characteristic of all BL Lac jets. This idea is supported by the modelling of the radiogalaxy emission through the spine-layer model (Tavecchio & Ghisellini 2008, 2014), which suggests that these jets are typically more powerful than those associated with the weakest BL Lac (rather, they resemble the BL Lacs of the intermediate, IBL, or low-synchrotron peak, LBL, category). These arguments motivated us to extend our previous work presented in Paper I, considering the possibility that the entire BL Lac population is a source of high-energy neutrinos. To this aim, we have to refine the simple description of the cosmic evolution we adopted in Paper I with a more complex, luminosity-dependent, evolution of the BL Lac luminosity function. We describe our neutrino emission model and the assumed cosmic evolution of BL Lacs in Section 2. We report the results in Section 3, in which we also present a list of the most probable candidates expected to be associated with the IceCube events. In Section 4, we conclude with a discussion.

Throughout the paper, the following cosmological parameters are assumed: $H_0 = 70$ km s^{-1} Mpc^{-1}, $\Omega_{\rm M} = 0.3$, $\Omega_{\Lambda} = 0.7$. We use the notation $Q = Q_X\, 10^X$ in cgs units.

2 SETTING THE STAGE

2.1 Neutrino emission

We calculate the neutrino emission from a single BL Lac following the scheme already adopted and described in Paper I. Here we just recall its basic features.

We assume a two-flow jet structure, with a fast spine (with bulk Lorentz factor $\Gamma_{\rm s}$) with cross-sectional radius R surrounded by the slower and thin layer (with $\Gamma_{\rm l} < \Gamma_{\rm s}$). The corresponding Doppler factors, denoting with $\theta_{\rm v}$ the observing angle, are $\delta_{\rm l,s} = [\Gamma_{\rm l,\,s}(1 - \beta_{\rm l,\,s}\cos\theta_{\rm v})]^{-1}$.

We further assume that the spine carries a population of high-energy CR (protons, for simplicity), whose luminosity in the spine frame (for which we use primed symbols) is parametrized by a cut-off power-law distribution in energy:

$$L'_{\rm p}(E'_{\rm p}) = k_{\rm p} E'^{-n}_{\rm p} \exp\left(-\frac{E'_{\rm p}}{E'_{\rm cut}}\right) \qquad E'_{\rm p} > E'_{\rm min} \tag{1}$$

with total (spine frame) luminosity $L'_{\rm p} = \int L'_{\rm p}(E'_{\rm p})\, {\rm d}E'_{\rm p}$. The cooling rate $t'^{-1}_{p\gamma}(E'_{\rm p})$ of protons with energy $E'_{\rm p}$ through the photomeson reaction with a target radiation field with numerical density $n'_{\rm t}(\epsilon)$ is given by (Atoyan & Dermer 2003, see also Dermer & Menon 2009):

$$t'^{-1}_{p\gamma}(E'_{\rm p}) = c \int_{\epsilon_{\rm th}}^{\infty} {\rm d}\epsilon\, \frac{n'_{\rm t}(\epsilon)}{2\gamma'^{2}_{\rm p}\epsilon^{2}} \int_{\epsilon_{\rm th}}^{2\epsilon\gamma'_{\rm p}} {\rm d}\bar{\epsilon}\, \sigma_{p\gamma}(\bar{\epsilon})\, K_{p\gamma}(\bar{\epsilon})\, \bar{\epsilon}, \tag{2}$$

where $\gamma'_{\rm p} = E'_{\rm p}/m_{\rm p}c^2$, $\sigma_{p\gamma}(\epsilon)$ is the photopion cross-section, $K_{p\gamma}(\epsilon)$ is the inelasticity and $\epsilon_{\rm th}$ is the threshold energy of the process. The photomeson production efficiency is measured by the factor $f_{p\gamma}$, defined as the ratio between the time-scales of the competing adiabatic and photomeson losses:

$$f_{p\gamma}(E'_{\rm p}) = \frac{t'_{\rm ad}}{t'_{p\gamma}(E'_{\rm p})}, \tag{3}$$

where $t'_{\rm ad} \approx R/c$.

The neutrino luminosity in the spine frame can thus be calculated as

$$E'_\nu L'_\nu(E'_\nu) \simeq \frac{3}{8}\min[1, f_{p\gamma}(E'_{\rm p})]\, E'_{\rm p} L'_{\rm p}(E'_{\rm p}), \tag{4}$$

where $E'_\nu = 0.05\, E'_{\rm p}$. The factor 3/8 takes into account the fraction of the energy going into ν and $\bar{\nu}$ (of all flavours).

The *observed* luminosity is derived taking into account the relativistic boosting, parametrized by the relativistic Doppler factor $\delta_{\rm s}$: $E_\nu L_\nu(E_\nu) = E'_\nu L'_\nu(E'_\nu)\, \delta_{\rm s}^4$ and $E_\nu = \delta_{\rm s} E'_\nu$.

We assume that the dominant population of soft photons – specifying $n'_{\rm t}(\epsilon)$ in equation (2) – is provided by the boosted layer radiation (we show in Paper I that the internally produced synchrotron photons provide a negligible contribution, thus making a one-zone model unable to reproduce the data, unless one allows for extremely large CR power). The spectrum of this component is modelled as a broken power law $L(\epsilon_{\rm l})$ with indices $\alpha_{1,\,2}$ and (observer frame, unprimed symbols) spectral energy distribution (SED) peak energy $\epsilon_{\rm o}$. The layer luminosity is parametrized by the total (integrated) luminosity – in the observer frame – $L_{\rm l}$.

As in Paper I we neglect the anisotropy of the layer radiation field in the spine frame (Dermer 1995). We also neglect the high-energy photons produced in the neutral pion decay $\pi^0 \rightarrow \gamma\gamma$.

2.2 Model parameters and scaling laws

Summarizing, our model is specified by the following 11 parameters: the jet radius, R, the spine and layer Lorentz factors $\Gamma_{\rm s}$ and $\Gamma_{\rm l}$, the observed layer radiative luminosity $L_{\rm l}$, the peak $\epsilon_{\rm o}$ of its energy distribution [in $\epsilon L(\epsilon)$], the spectral slopes α_1 and α_2 of $L_{\rm l}(\epsilon)$, the spine comoving CR luminosity L'_p, the CR power-law index n, the minimum and the cut-off energy $E'_{\rm min}$, $E'_{\rm cut}$.

Admittedly, the set of free parameters is relatively large. However, not all parameters have the same importance in determining the shape and the level of the resulting neutrino spectrum. For instance, the slopes of the layer spectrum α_1 and α_1 have a very minor impact on the resulting spectrum (as long as their value is within the range usually considered), which is instead mostly driven by the CR distribution. Moreover, several of these parameters – in particular those related to jet structure – can be tuned to the values inspired by observations and previous applications of the structured jet model to blazars and radiogalaxies (see also Paper I). With these motivations and for definiteness in the following, we assume $\Gamma_{\rm s} = 15$, $\Gamma_{\rm l} = 2$, a jet radius $R = 10^{15}$ cm and a layer spectrum with slopes $\alpha_1 = 0.5$ and $\alpha_2 = 1.5$.

More important is the role of the peak energy of the layer emission $\epsilon_{\rm o}$ which regulates, through the photopion threshold condition $E'_{\rm p}\epsilon'_{\rm t} > m_\pi m_{\rm p} c^4$, the possible values of the minimum CR energy and the position of the maximum of the neutrino emitted luminosity. In fact, increasingly larger values of $\epsilon_{\rm o}$ allow for lower values of $E'_{\rm p,min}$ and thus lower energies of the produced neutrinos. On the other hand, due to the steep CR distribution, decreasing $E'_{\rm p,min}$ leads to increase the CR power required to produce a given neutrino output.

In Paper I we considered two possible realizations of the model, characterized by two different values of the layer peak energy. We showed that to satisfactorily reproduce the low-energy data points around 100 TeV, one has to assume a layer emission peaking in the UV band, $\epsilon_{\rm o} \approx 400$ eV. Although we cannot exclude that the layer peak energy varies across the BL Lac population – therefore determining a more complicated neutrino emission – for simplicity in the following we adopt this value for our reference model.

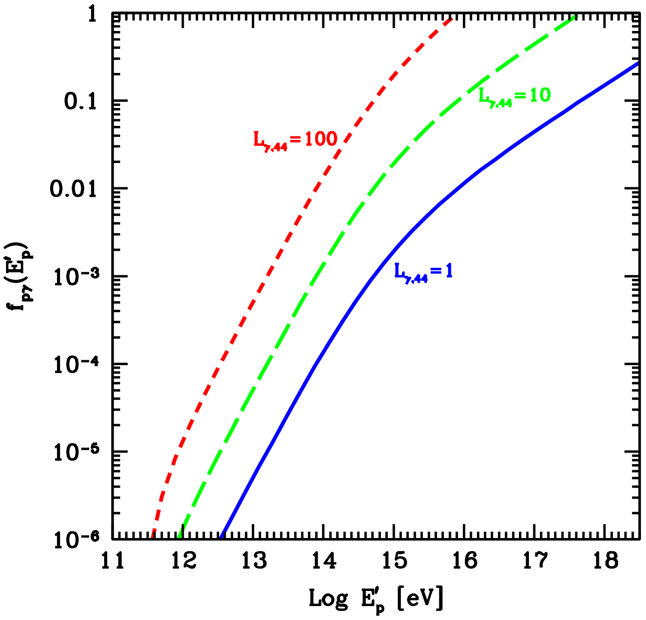

Figure 1. Photopion production efficiency, $f_{p\gamma}$, as a function of the energy (in the jet spine frame) for protons carried by the spine scattering off the layer radiation field, for a BL Lac γ-ray luminosity $L_\gamma = 10^{44}$ erg s^{-1} (solid blue line), $L_\gamma = 10^{45}$ erg s^{-1} (long dashed green line) and $L_\gamma = 10^{46}$ erg s^{-1} (dashed red line).

For both the CR luminosity $L'_{\rm p}$ and the layer radiative luminosity $L_{\rm l}$, we assume, as a physically motivated working hypothesis, a linear dependence on the jet power, $P_{\rm jet}$ – i.e. constant efficiencies. In turn, we assume that $P_{\rm jet}$ is well traced by the observed γ-ray 0.1–100 GeV luminosity, L_γ, as supported by the modelling of blazar SED (e.g. Ghisellini et al. 2014). We normalize the values of $L'_{\rm p}$ and $L_{\rm l}$ to the values corresponding to the weakest sources, corresponding to $L_\gamma = 10^{44}$ erg s^{-1}. Therefore, we assume

$$L'_{\rm p} = L'_{\rm p,o}\,\frac{L_\gamma}{10^{44}\ {\rm erg\ s^{-1}}}; \quad L_{\rm l} = L_{\rm l,o}\,\frac{L_\gamma}{10^{44}\ {\rm erg\ s^{-1}}}. \tag{5}$$

For the layer we adopt the value used in Paper I, $L_{\rm t,\,o} = 2 \times 10^{44}$ erg s^{-1}, while $L'_{\rm p,o}$ is left as a free parameter, Note that what matters for the resulting neutrino luminosity is the product of these two parameters, not their single values. Therefore, the results shown below could be obtained for different choices of $L_{\rm t,\,o}$ and $L'_{\rm p,o}$. Our specific choice somewhat maximizes the layer luminosity $L_{\rm t,\,o}$, allowing us to maximize the photomeson efficiency and thus to minimize the CR power $L'_{\rm p,o}$.

The parameters specifying the CR distribution are left free and adjusted to reproduce the observations. In principle, one could assume a dependence of these parameters on the jet power. However, in the absence of a clear physical motivation, a detailed choice is somewhat arbitrary. Moreover, as we will discuss below, the neutrino diffuse emission is dominated, in our scheme, by the most powerful sources. In this sense, the neutrino spectrum is mostly dictated by the CR parameters associated with sources of a given luminosity and thus a possible luminosity dependence is only relatively relevant for our results. The value of $f_{p\gamma}(E'_{\rm p})$ for the assumed set of parameters is shown in Fig. 1. Note the large efficiency ($f_{p\gamma} > 0.1$) characterizing the most powerful sources for proton energies corresponding to the neutrinos detected by IceCube. For these sources, $f_{\rm p\gamma}$ even reaches 1 for $E'_{\rm p}$ of few PeV, implying that CR of these energies effectively cool through photomeson losses.

Given the assumed linear scaling of CR and layer luminosities with the jet power, the neutrino luminosity – proportional to their product – will scale as $L_\nu \propto L'_{\rm p} L_{\rm t} \propto L_\gamma^2$. Alternatively, this can be expressed by the fact that the efficiency of the neutrino production, $\eta_\nu \equiv L_\nu / P_{\rm jet}$, increases with the jet power (and thus with the γ-ray luminosity), $\eta_\nu \propto L_\gamma$. We will see that this fact implies that, despite that the cosmic density of sources decreases with their γ-ray luminosity (i.e. a decreasing luminosity function), the cumulative cosmic neutrino output is dominated by the most powerful – but rare – sources.

2.3 Diffuse intensity

The cumulative diffuse neutrino intensity deriving from the entire population of BL Lacs is evaluated as

$$E_\nu I(E_\nu) = \frac{cE_\nu^2}{4\pi H_o} \int_0^{z_{\rm max}} \int_{L_{\gamma,1}}^{L_{\gamma,2}} \frac{j[L_\gamma, E_\nu(1+z), z]}{\sqrt{\Omega_{\rm M}(1+z)^3 + \Omega_\Lambda}} \, {\rm d}L_\gamma \, {\rm d}z, \quad (6)$$

in which the luminosity-dependent comoving volume neutrino emissivity j is expressed by the product of the comoving density of sources with a given γ-ray luminosity, provided by the luminosity function $\Sigma(L_\gamma, z)$, and the corresponding source neutrino luminosity:

$$j(L_\gamma, E_\nu, z) = \Sigma(L_\gamma, z) \, \frac{L_\nu(E_\nu)}{E_\nu}. \quad (7)$$

Equation (6) is a generalization of the relation used in Paper I, which was suitable for a population of sources with a unique luminosity.

We derive $\Sigma(L_\gamma, z)$ using the luminosity function and the parameters for its luminosity-dependent evolution for BL Lacs derived by Ajello et al. (2014) using *Fermi*/LAT data. The local (i.e. $z = 0$) luminosity function is described by

$$\Sigma(L_\gamma, z=0) = \frac{A}{\ln(10) L_\gamma} \left[\left(\frac{L_\gamma}{L_*} \right)^{\gamma 1} + \left(\frac{L_\gamma}{L_*} \right)^{\gamma 2} \right]^{-1} \quad (8)$$

with $A = 3.4 \times 10^{-9}$ Mpc^{-3}, $\gamma 1 = 0.27$, $\gamma 2 = 1.86$ and $L_* = 2.8 \times 10^{47}$ erg s^{-1}. This luminosity function evolves with z as

$$\Sigma(L_\gamma, z) = \Sigma(L_\gamma, z=0) \times e(L_\gamma, z), \quad (9)$$

where[1]

$$e(L_\gamma, z) = \left[\left(\frac{1+z}{1+z_c(L_\gamma)} \right)^{-p1(L_\gamma)} + \left(\frac{1+z}{1+z_c(L_\gamma)} \right)^{-p2} \right]^{-1}, \quad (10)$$

and the functions $z_c(L_\gamma)$ and $p1(L_\gamma)$ are specified by

$$z_c(L_\gamma) = z_c^* \times (L_\gamma / 10^{48} \, {\rm erg\, s^{-1}})^\alpha, \quad (11)$$

$$p1(L_\gamma) = p1^* + \tau \times \log(L_\gamma / 10^{46} \, {\rm erg\, s^{-1}}). \quad (12)$$

The best-fitting parameters derived by Ajello et al. (2014) are $p2 = -7.4$, $z_c^* = 1.34$, $\alpha = 4.53 \times 10^{-2}$, $p1^\star = 2.24$ and $\tau = 4.92$.

This parametrization captures the basic features of the γ-ray emitting BL Lac evolution. In particular, low-luminosity sources ($L_\gamma < 10^{45}$ erg s^{-1}) are characterized by a negative evolution (i.e. a density decreasing with z), while sources of higher luminosity display a null or positive evolution.

Table 1. Parameters for the two realizations of the model shown in Fig. 2. The three columns report the normalization of the CR luminosity, the minimum and the cut-off energy of the CR energy distribution.

Model	$L'_{\rm p,o}$ (erg s^{-1})	$E'_{\rm min}$ (eV)	$E'_{\rm cut}$ (eV)
All	3×10^{40}	2×10^{13}	3×10^{15}
Low power	3×10^{41}	2×10^{13}	2.3×10^{15}

We consider that the BL Lac γ-ray luminosity is in the range 10^{44} erg s^{-1} $< L_\gamma <$ 10^{46} erg s^{-1}. Note that in the *Fermi* second LAT AGN catalogue (2LAC; Ackermann et al. 2011), there are sources classified as BL Lac objects with even larger L_γ, as also assumed in the population study of Ajello et al. (2014). However, as discussed in Ghisellini et al. (2011, see also Giommi, Padovani & Polenta 2013; Ruan et al. 2014), these are instead intermediate objects between FSRQ and BL Lacs or even misclassified FSRQ whose beamed non-thermal continuum is so luminous to swamp the broad emission lines. We suppose that the jets of these sources do not develop an important layer and therefore we do not consider them as neutrino emitters.

The assumed maximum luminosity is much below the break luminosity L_*. The local luminosity function, equation (8), can thus be well approximated by a single power law, $\Sigma(L_\gamma, z=0) \propto L_\gamma^{-(\gamma_1+1)}$. Recalling the relation between the neutrino and the γ-ray luminosity ($L_\nu \propto L_\gamma^2$), the neutrino luminosity density (equation 7) can also be expressed as a function of the sole γ-ray luminosity. Therefore, we can express the contribution of the sources with a given γ-ray luminosity to the total neutrino background as

$$I(L_\gamma) \propto L_\gamma \, j(L_\gamma) \propto L_\gamma \, \Sigma(L_\gamma, z) \, L_\nu \propto L_\gamma^{-\gamma_1+2} \quad (13)$$

from which $I(L_\gamma) \propto L_\gamma^{1.73}$, i.e. the resulting integral neutrino flux is dominated by the most powerful sources.

3 RESULTS

3.1 Cumulative intensity

We apply the model described above to reproduce the observed neutrino intensity. As noted above, the only free parameters of the model are those specifying the proton energy distribution and the total CR luminosity normalization: n, $E'_{\rm min}$, $E'_{\rm cut}$ and $L'_{\rm p,o}$. First, we consider the case in which the entire BL Lac population is characterized by the presence of a structured jet, fixing $L_{\gamma,2} = 10^{46}$ erg s^{-1} in equation (6). For the parameters reported in the first row of Table 1, we obtain the diffuse spectrum shown by the solid black line in Fig. 2 (upper panel), to be compared with the reported IceCube data points from Aartsen et al. (2014). The abrupt cut-off at low energy is an artefact due to the assumed abrupt truncation of the CR energy distribution at low energy.

The grey lines show the contributions from BL Lacs in two different ranges of luminosity, namely 10^{44}–10^{45} erg s^{-1} (dashed) and 10^{45}–10^{46} erg s^{-1} (long dashed). As expected from the considerations above (Section 2.3), the total emission is dominated by the most luminous sources, although their density is much smaller than that of the low-luminosity ones.

The high-energy cut-off of the CR distribution is robustly fixed to $E'_{\rm cut} = 3$ PeV by the IceCube upper limits at high energy. A larger value would lead to overpredict the flux above few PeV.

---

[1] The sign of the exponents $p1$ and $p2$ in Ajello et al. (2014) is incorrect (Ajello, private communication).

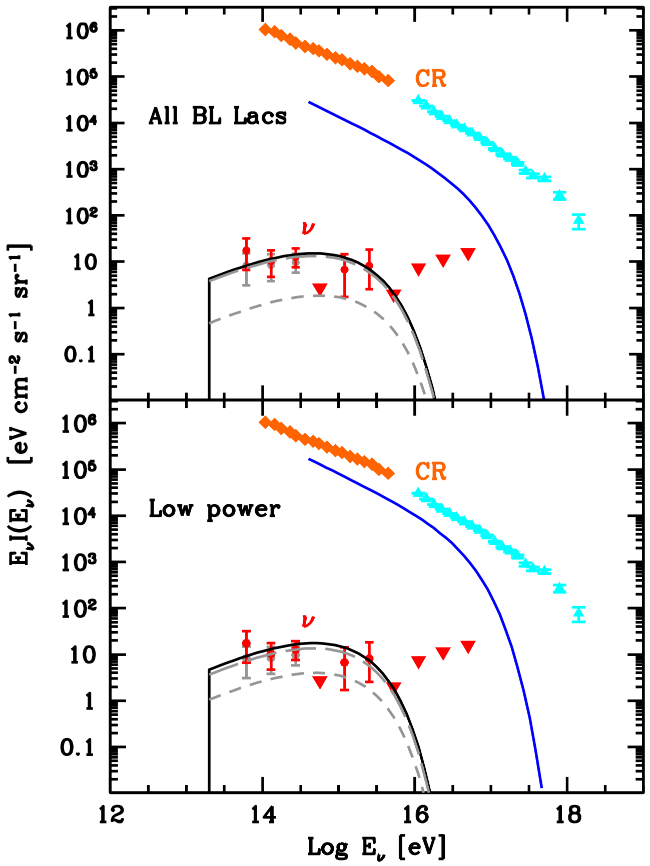

Figure 2. Upper panel: measured diffuse intensities of high-energy neutrinos (red symbols, from Aartsen et al. 2014). Red triangles indicate upper limits. Grey data points show the fluxes for an increase of the prompt atmospheric background to the level of 90 per cent CL limit. The black solid line reports the diffuse neutrino intensity calculated assuming that all the BL Lac jets have a spine-layer structure. Grey lines report the contributions from sources with 10^{44} erg s^{-1} $< L_\gamma <$ 10^{45} erg s^{-1} (dashed) and 10^{45} erg s^{-1} $< L_\gamma <$ 10^{46} erg s^{-1} (long dashed). The blue lines report the corresponding CR intensities, assuming efficient escape from the jet. Orange (Apel et al. 2012) and cyan (Chen 2008) data points show the observed high-energy CR spectrum. Lower panel: same as the upper panel but considering only the sources with $L_\gamma < 10^{45}$ erg s^{-1}. Grey lines show the contribution of sources with 10^{44} erg s^{-1} $< L_\gamma < 3 \times 10^{44}$ erg s^{-1} (dashed) and 3×10^{44} erg s^{-1} $< L_\gamma <$ 10^{45} erg s^{-1} (long dashed).

Although clearly this value has been obtained through a fine-tuning with the data, we note that it is consistent with the expectation for the most powerful sources, for which the CR energy is likely limited by photomeson losses (more in Section 3.2). The value of the minimum CR energy $E'_{\rm min}$ is instead less constrained. The lowest energy IceCube data point at ≈100 TeV allows us to limit $E'_{\rm min}$ from above, $E'_{\rm min} \lesssim 20 \times E_\nu/\delta_{\rm s} \approx 10^{14}$ eV (we ignore the cosmological redshift). The curves in Fig. 2 have been derived by assuming $E'_{\rm min} = 2 \times 10^{13}$ eV, although lower values are allowed. The flat spectrum points to a relatively soft CR spectrum, $n = 2.8$.

In the lower panel of Fig. 2, we report the case, similar to that discussed in Paper I, in which only the jets of the weak BL Lacs – operatively defined as the sources with $L_\gamma < 10^{45}$ erg s^{-1} – develop a layer. The CR power for a given γ-ray luminosity, $L'_{\rm p,o}$, increases by a factor of 10 with respect to the previous case.

In Fig. 2, we also show the cumulative CR flux from BL Lacs (blue lines) assuming efficient escape from the jet and efficient penetration within the Milky Way. For the case of all BL Lacs, the flux is well below the measured level. For the case of HBL alone, the flux is close to the limit fixed by the level recorded at the Earth. This is because, if only low-power BL Lacs have to reproduce the neutrino flux, they must contain a number of energetic CR which is greater than if BL Lacs of all powers contribute, since, as noted before, the photopion production efficiency $f_{p\gamma}$ – and hence the neutrino emission efficiency – increases with the jet power (or, equivalently, with the γ-ray luminosity) – i.e. low-power jets are less efficient than high-power jets in producing neutrinos. For our two models, the contribution of the BL Lacs to the CR in the 10^{15}–3×10^{16} eV energy range is of the order of ∼5 and ∼50 per cent for the 'All' and the 'Low-power' case, respectively.

3.2 CR power

The CR luminosity required to match the observed flux is relatively limited. The γ-ray luminosity-dependent beaming-corrected power in CR (similar to that valid for photons; e.g. Celotti & Ghisellini 2008):

$$P_{\rm CR} = \frac{L'_{\rm p}\,\delta_{\rm s}^4}{\Gamma_{\rm s}^2} = L'_{\rm p,o} L_{\gamma,44}\,\frac{\delta_{\rm s}^4}{\Gamma_{\rm s}^2} \qquad (14)$$

is $P_{\rm CR} \simeq 2 \times 10^{43} L_{\gamma,\,44}$ erg s^{-1} ('All' case) and $P_{\rm CR} \simeq 2 \times 10^{44} L_{\gamma,\,44}$ erg s^{-1} ('Low-power' case). This value can be compared to the beaming-corrected radiative luminosity, which for blazars can be directly related to the observed γ-ray luminosity (Sbarrato et al. 2012), $P_{\rm rad} \approx 3 \times 10^{42} L_{\gamma,44}^{0.78}$ erg s^{-1}. The (γ-ray luminosity-dependent) ratio between the two quantities is thus $\xi = P_{\rm CR}/P_{\rm rad} \approx 5\,L_{\gamma,44}^{0.22}$ and $\approx 50\,L_{\gamma,44}^{0.22}$ for the two cases. These values should be compared to $\xi \approx 100$ assumed by Murase et al. (2014) – although the possible existence of a curved CR distribution as that discussed by Dermer et al. (2014) should allow one to reduce such a large value.

Since for blazar jets the ratio between the radiative and the kinetic power (calculated assuming a composition of one *cold* proton per emitting electron) is $P_{\rm rad}/P_{\rm jet} \approx 0.1$ (e.g. Nemmen et al. 2012; Ghisellini et al. 2014), we can also assess the ratio between the jet power (calculated neglecting the contribution of CR) and the CR power, i.e. $P_{\rm CR}/P_{\rm jet} \approx 0.5\,L_{\gamma,44}^{0.22}$ for the 'All' case and 10 times larger for the 'Low-power' case. Therefore, even in the most conservative case, the jet should be able to channel a sizeable part of its kinetic power into CR acceleration. As a consequence, the total jet power should increase by a corresponding amount with respect to the current estimates.

3.3 Neutrino point sources

Having calculated the expected cumulative neutrino flux, we can also derive the expected number of events detectable by IceCube from a given BL Lac object. This is particularly valuable in view of the identification of the possible astrophysical counterparts of the detected neutrinos and to test our model.

To this aim, first of all we calculate the theoretical differential neutrino number flux at the Earth from a generic source of neutrino luminosity L_ν at redshift z as

$$\phi(E_\nu) \equiv \frac{{\rm d}N}{{\rm d}t\,{\rm d}E_\nu\,{\rm d}A} = \frac{L_\nu[E_\nu(1+z)]}{4\pi d_L^2\,E_\nu}, \qquad (15)$$

where $d_{\rm L}$ is the luminosity distance. We derive the expected IceCube rate convolving the flux with the energy-dependent IceCube

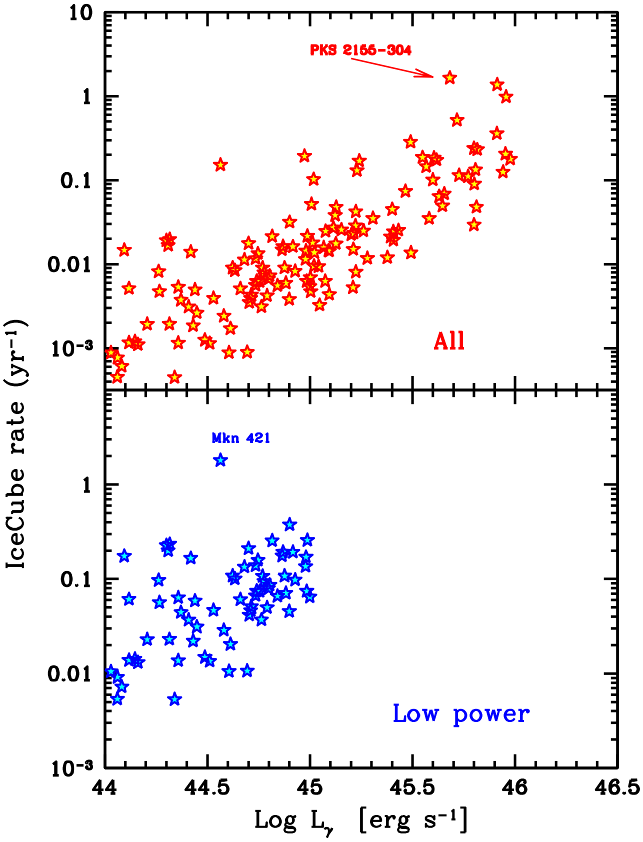

Figure 3. Expected IceCube count rate (events/year) for the 2LAC BL Lac as a function of the γ-ray luminosity for the 'All' (upper panel) and the 'Low-power' (lower panel) scenario, respectively.

effective area $A_{\rm eff}$. We used the angle-averaged point-source effective area provided by Yacobi, Guetta & Behar (2014). Note that, due to different cuts and analysis thresholds, this effective area is larger (by a factor of $\approx$5) than the effective area associated with the IceCube analysis of the diffuse background given in Aartsen et al. (2013a). Finally, we derive the number of events expected with an exposure of 3 years (corresponding to an effective exposure of $T_{\rm exp} = 998$ d):

$$N_\nu = T_{\rm exp} \int A_{\rm eff}(E_\nu)\phi(E_\nu)\,{\rm d}E_\nu. \qquad (16)$$

For consistency, we first checked that our two models represented in Fig. 2 provide about 30 events detected in 3 years (Aartsen et al. 2014). We then applied the procedure using the BL Lacs belonging to the 2LAC[2] (Ackermann et al. 2011) with measured redshift. For each source, the γ-ray luminosity is derived converting the flux provided by the 2LAC using the procedure described in Ghisellini, Maraschi & Tavecchio (2009). The γ-ray luminosity is then converted into the luminosity in neutrinos $L_\nu(E_\nu)$ according to our model. The resulting event rates ($N_\nu/T_{\rm exp}$ in units of yr^{-1}) for the sources, as a function of L_γ, are reported in Fig. 3 for the two scenarios. The numbers of events for the exposure of 998 d N_ν for the five brightest sources and for the two possible scenarios explored above are reported in Table 2.

For the 'All' scenario, the brightest three to four sources are characterized by a rate sufficient to allow the detection of several events with a relatively prolonged exposure. The most probable candidate is PKS 2155−304 (see below). On the other hand, if only low-power BL Lacs are considered, the situation is different, with one source – Mrk 421 – expected to be clearly detectable and with all the other sources with a smaller flux, providing $N_\nu/T_{\rm exp} < 0.5$ yr^{-1}.

Table 2. List of the BL Lacs and the expected neutrino counts for an exposure of 3 yr and the two scenarios described in the text.

Source	z	N_ν (998 d)
	All	
PKS 2155−304	0.116	4.5
PKS 0447−439	0.205	3.7
PKS 0301−243	0.26	2.7
1H 1013+498	0.212	1.4
S4 0954+65	0.367	1.0
	Low power	
Mrk 421	0.031	4.9
1ES 0806−05	0.137	1.0
RX J 0159.5+1047	0.195	0.7
1ES 1959+650	0.047	0.6
1ES 2322−409	0.1735	0.5

An obvious *caveat* is in order when considering this result. This calculation, although applied to single sources, is built on our results based on the *averaged* characteristics of the BL Lac population (besides our model assumptions). Furthermore, the γ-ray luminosity of the 2LAC is an average over 2 years of observations. Given these limits, our procedure cannot consider source peculiarities or mid-term variability, particularly relevant for the high-energy emission of luminous BL Lac objects (e.g. Abdo et al. 2010).

Given these limitations, it is however possible to note a clear difference between the two cases: in the 'All' case there is a bunch of relatively bright neutrino BL Lacs – those with the highest power. For the 'Low-power' case, instead, Mrk 421 largely dominates over the other sources. A remark concerns the case PKS 2155−304, the first entry in Table 2 for the 'All' case, which is the only HBL of this list. Indeed, as we noted above, the neutrinos reaching the Earth are preferentially produced by the most powerful sources which preferentially are of the IBL or LBL type (e.g. Ackermann et al. 2011; Giommi et al. 2012). PKS 2155−304 is clearly an outlier of this general trend, displaying an SED typical of HBL (i.e. the synchrotron peak in the soft X-ray band) but with a luminosity much larger than that of the averaged HBL population. Given the link that we assumed between the electromagnetic and neutrino output, this peculiarity shows up also in the neutrino window. In Fig. 4, we report in detail the SED and the expected neutrino output for this source. In the SED, we also report the IceCube sensitivity curve for 3 years, scaling that provided in Tchernin et al. (2013) for one year and about half of the detector (IC-40 configuration). Clearly, the flux limit is very close to that theoretically expected.

Recently, Ahlers & Halzen (2014) performed a calculation aimed to assess the possibility to single out neutrino sources with IceCube, considering different possible source scenarios and taking into account the details of the IceCube instrument (e.g. background, statistics). They also consider blazars as possible sources, adopting the local density and the cosmological evolution valid for the most powerful blazars, i.e. FSRQ. Comparing the neutrino flux they derived for single sources with the upper limits on the flux of the weak BL Lac Mrk 421 and Mrk 501, they conclude that a blazar origin is disfavoured. However, as said, their calculations are clearly tuned for FSRQ, not BL Lacs, which display quite different cosmological

---

[2] http://www.asdc.asi.it/fermi2lac/

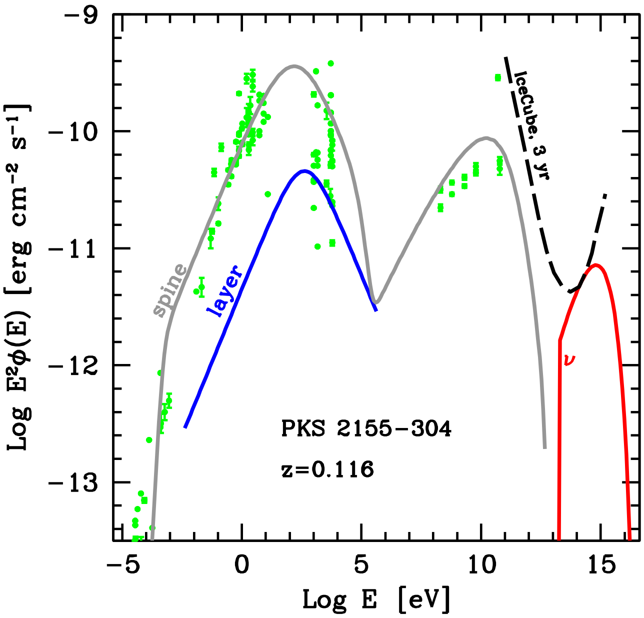

Figure 4. SED of PKS 2155−304 (green points – taken from http://www.asdc.asi.it – and solid grey line). The red solid line shows the expected neutrino emission expected in our model for the 'All BL Lac' case. The blue line tracks the corresponding layer emission. The black dashed line marked 'IceCube, 3 yr' displays the estimated flux limit for IceCube, obtained scaling the sensitivity curve provided in Tchernin et al. (2013).

density and evolution. Indeed, a calculation based on the BL Lac demography provides results compatible to those presented here (Ahlers, private communication.).

4 DISCUSSION

We have presented an extension of the scenario envisaging the production of high-energy neutrinos in the structured jets of BL Lac objects sketched in Paper I. The key ingredient is the relativistic boosting of the radiation produced in the layer in the spine frame (Ghisellini et al. 2005; Tavecchio & Ghisellini 2008), which entails the increased efficiency of the photopion reactions and the following neutrino emission. We stress that the synchrotron photons produced in the spine provide a rather small contribution to the total density of soft target photons. In the absence of a layer – in one-zone models – one should thus adopt larger CR luminosities to reach the level of the neutrino diffuse flux (see also Murase et al. 2014).

The observational evidence supporting the idea that BL Lac (and radiogalaxy) jets are structured outflows – i.e. with a faster spine surrounded by a slower layer – is steadily accumulating. The deceleration of the flow after the blazar region expected for this configuration offers the simplest explanation of the anomalous lower apparent speeds inferred for jets of TeV emitting BL Lac through VLBI observation (Piner & Edwards 2004; Piner, Pant & Edwards 2008). Likely, a spine-layer system is the most natural description of the limb brightening displayed by several BL Lac (Giroletti et al. 2004, 2008; Piner, Pant & Edwards 2010; Piner & Edwards 2014) and radiogalaxy (e.g. Müller et al. 2014; Nagai et al. 2014) jets at VLBI resolutions. Strong independent – although indirect – support is provided by arguments from the unification scheme of BL Lacs and Fanaroff–Riley type I (FR I) radiogalaxies (e.g. Chiaberge et al. 2000; Meyer et al. 2011; Sbarrato et al. 2014). Indeed, while large Lorentz factors ($\Gamma \approx 10$–20) are required to model the BL Lac emission (e.g. Tavecchio et al. 2010), the emission properties and the number density of radiogalaxies instead favour low ($\Gamma \approx 3$–5) bulk Lorentz factors. The structure jet scenario easily solves this problem: depending on the jet viewing angle, large or low Lorentz factors are inferred for BL Lac (dominated by the spine) or radiogalaxies (for which the layer contributes most to the emission), respectively.

There is relatively small number of cases for which some constraints to the structural parameters of the layer can be derived (e.g. Tavecchio & Ghisellini 2008, 2014). In our work, we assumed a phenomenological view, tuning the layer properties (bulk Lorentz factor, emitted spectrum) so that we can reproduce at best the observed neutrino flux. An improvement of present knowledge could help in better test our proposal.

One is naturally led to wonder whether misaligned BL Lacs – i.e. FR I radiogalaxies, according to the classical unification scheme for radio-loud AGN (e.g. Urry & Padovani 1995) – could also contribute to the observed neutrino background (see also Becker Tjus et al. 2014). In this case, one expects that the close-by radiogalaxies Cen A, M87 and NGC 1275 – also observed to emit TeV photons (Aharonian et al. 2006, 2009; Aleksić et al. 2012) – should be optimal candidates for a direct association with IceCube events (recall also that Cen A is also possibly associated with a handful of UHECR detected by Auger; Abraham et al. 2007). For all three sources, however, quite stringent upper limits are derived (Aartsen et al. 2013b). In the structured jets scenario adopted here, the electromagnetic emission from the inner jet of radiogalaxies (at least at high energies, see below) is likely to be dominated by the layer, since, due to the large viewing angle, the more beamed spine radiation is deboosted as observed from the Earth. Analogously, we expect that possible neutrino emission from the layer would dominate over that of the spine in case of misaligned jets. As for the inverse Compton emission (e.g. Tavecchio & Ghisellini 2008), the dominant radiation field for the photopion reaction is expected to be that of the spine, boosted in the layer frame by the relative motion. For M87 and NGC 1275, the application of the spine-layer scenario (Tavecchio & Ghisellini 2008, 2014) suggests that the high-energy γ-ray component is produced in the layer, while the low-energy non-thermal emission is rather due to the (deboosted) spine emission. In this case, we therefore have a direct handling on the spine radiation field. For all the aforementioned radiogalaxies, this low-energy component peaks in the IR band, around $\epsilon_{\rm o} \approx 0.1$ eV. Therefore, in order to allow the photomeson reaction, proton energies should exceed (we neglect the small Doppler shift) $E_{\rm p} \gtrsim m_\pi m_{\rm p} c^4/\epsilon_{\rm o} \approx 10^{18}(\epsilon_{\rm o}/0.1\ {\rm eV})^{-1}$ eV, implying that the resulting neutrinos have energies exceeding $E_\nu \gtrsim 50$ PeV, well above the energies of neutrinos considered here. If such high energy for protons is attainable, upcoming new detectors extending beyond the IceCube band (ARA, Allison et al. 2012; ARIANNA, Barwick 2007; ANITA, Gorham et al. 2009; EVA, Gorham et al. 2011) could thus be able to detect neutrinos from the layer of nearby radiogalaxies.

An attractive feature of our scenario, especially in the case for which the entire BL Lac population contributes to the observed flux, is the moderate required power in CR. Indeed, while it is typically assumed that the CR luminosity greatly exceeds that in radiation (e.g. Murase & Nagataki 2006; Murase et al. 2014), we found that a ratio $P_{\rm CR}/P_{\rm rad} \approx 5$ can match the observed flux. In turn, the ratio between the CR power and the kinetic power – as derived through the modelling of the observed emission with standard leptonic models, e.g. Ghisellini et al. (2014) – is $P_{\rm CR}/P_{\rm jet} \lesssim 1$. In case of fast cooling of the accelerated electrons, $P_{\rm CR}/P_{\rm rad}$ directly provides a measure of

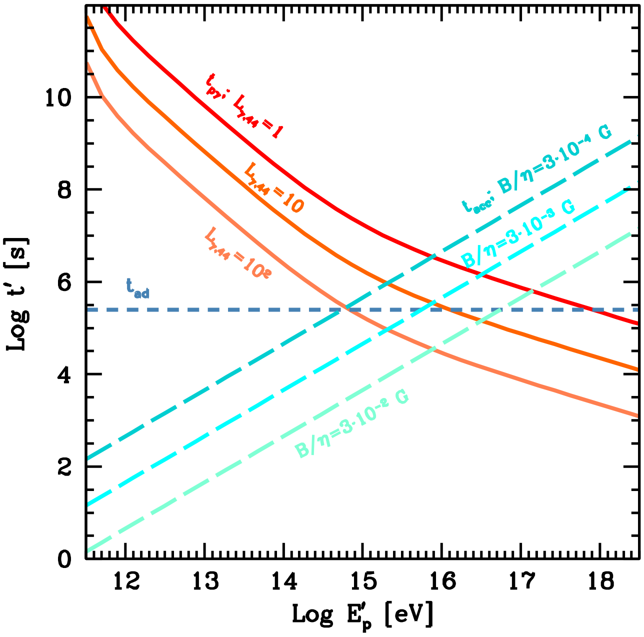

Figure 5. Acceleration and cooling time-scales (in the spine rest frame) expected for high-energy protons on BL Lac jets. Red lines show the photomeson time-scale $t_{p\gamma}$ for three different values of the γ-ray luminosity. Blue lines show an estimate of the acceleration time-scale for three values of the ratio of magnetic field to acceleration efficiency, B/η. The horizontal line is the adiabatic time-scale for a radius $R = 10^{15}$ cm.

the electron-to-proton luminosity ratio, $f_{\rm e} \approx P_{\rm rad}/P_{\rm CR}$. Theoretical expectations indicate values $f_{\rm e} \ll 1$, (e.g. Becker Tjus et al. 2014 and references therein), consistent with our findings. The fact that the CR power can be a sizeable fraction of the jet power could perhaps be linked to the deceleration of the jet from sub-pc to pc scale as inferred from VLBI observations (e.g. Piner & Edwards 2014). We also recall that propagating CR beams produced by BL Lac jets have been invoked to explain several peculiarities of low-power BL Lac jets (the so-called extreme HBL), in particular their hard and slowly variable TeV emission (e.g. Essey et al. 2010; Murase et al. 2012; Aharonian et al. 2013; Tavecchio 2014).

It should be remarked that the CR power sensitively depends on the minimum energy. In our modelling, we assumed $E'_{\rm min} \sim 10^{13}$ eV, as limited by the observed low-energy data points. Lower values are not excluded, of course, possibly increasing the energy budget. A related point concerns the required maximum CR energy. The IceCube upper limits robustly fixed the (spine rest frame) maximum energy to few PeV.

As noted above, the IceCube upper limits above 10 PeV robustly constrain the maximum energy of the parent CR to few PeV. Since, at least in the 'All' case, the photomeson efficiency $f_{p\gamma}$ can be close to 1 for the most powerful sources, it is tempting to relate the derived maximum energies to the equilibrium between losses and gains suffered by CR, expressed by the equality between cooling and acceleration time-scales $t_{\rm cool} \approx t_{\rm acc}$. In Fig. 5, we show the characteristic cooling and acceleration time-scales for different parameters (see e.g. Aharonian 2000). Photomeson cooling times are shown for three different values of the γ-ray luminosity. The acceleration time-scale is parametrized by the Larmor radius of the accelerated CR, r_L: $t'_{\rm acc}(E'_{\rm p}) = \eta\, r_L/c \simeq 1.36 \times 10^2 \eta E_{15} B^{-1}$ s. The parameter η – depending on the details of the acceleration process and microphysical parameters – is not well known (e.g. Rieger, Bosch-Ramon & Duffy 2007) but it should be in the range η = 10–100. We report three different curves, corresponding to values of the ratio B/η bracketing values suitable for BL Lac jets. Adiabatic losses are accounted for by using the adiabatic cooling time expected from jet expansion (Tavecchio 2014). Considering the most powerful jet, $L_\gamma = 10^{46}$ erg s^{-1}, and above $E'_{\rm p} \approx 10^{14}$ eV the cooling time is ruled by photomeson losses. The expected maximum energies for the considered range (defined by the intersection of the curves for photomeson losses and those for acceleration) of B/η is $E'_{\rm p} \sim 3 \times 10^{14}$–$10^{16}$ eV. Low-power sources, instead, are characterized by a less important photomeson cooling. In this case, the dominating losses are the adiabatic ones, defining a similar range $E'_{\rm p} \sim 3 \times 10^{14}$–$3 \times 10^{16}$ eV. In both cases, typical energies around the PeV range should be expected.

We provided a list of the sources with the largest expected neutrino flux, which are the best candidates to be detected as point sources by IceCube. The kind and the characteristics of the sources are quite different in the two scenarios. In the case in which neutrino emission occurs in all the BL Lac population, the brightest sources are those with powerful jets (IBL and LBL type) located at relatively large redshift ($z \sim 0.2$). The most probable source is PKS 2155−304, an HBL with an atypically large luminosity. In the case in which, instead, only low-power jets have an efficient layer, the most probable sources associated with neutrino events are HBL at low redshift. In both cases, we expect that the brightest sources could have several associated neutrinos in the next few years. If BL Lac objects are the sources dominating the extragalactic neutrino sky, our model can thus be effectively tested by a more extended IceCube exposure and the two options that we presented could be effectively distinguished.

In this work, we have assumed that the entire diffuse emission is related to BL Lacs, but we cannot exclude that the more powerful – but more rare – FSRQ contribute to or even dominate the neutrino background. However, as discussed by Murase et al. (2014) and Dermer et al. (2014), the dominant UV ambient radiation field surrounding the jet in FSRQ leads to predict that the bulk of the neutrino output should be emitted above the PeV range. More accumulated data will also permit to assess the role of FSRQ.

ACKNOWLEDGEMENTS

We thank T. Montaruli for discussions and an anonymous referee for a constructive report. FT acknowledges contribution from a grant PRIN–INAF–2014. Part of this work is based on archival data and online services provided by the ASI Science Data Center.

REFERENCES

Aartsen M. G. et al., 2013a, Science, 342, 1242856
Aartsen M. G. et al., 2013b, ApJ, 779, 132
Aartsen M. G. et al., 2014, Phys. Rev. Lett., 113, 101101
Abdo A. A. et al., 2010, ApJ, 722, 520
Abraham J. et al., 2007, Science, 318, 938
Ackermann M. et al., 2011, ApJ, 743, 171
Aharonian F. A., 2000, New Astron., 5, 377
Aharonian F. et al., 2006, Science, 314, 1424
Aharonian F. et al., 2009, ApJ, 695, L40
Aharonian F., Essey W., Kusenko A., Prosekin A., 2013, Phys. Rev. D, 87, 063002
Ahlers M., Halzen F., 2014, Phys. Rev. D, 90, 043005
Ahlers M., Murase K., 2014, Phys. Rev. D, 90, 023010
Ajello M. et al., 2014, ApJ, 780, 73
Aleksić J. et al., 2012, A&A, 539, L2
Allison P. et al., 2012, Astropart. Phys., 35, 457

Anchordoqui L. A. et al., 2014, J. High Energy Astrophys., 1, 1

Apel W. D. et al., 2012, Astropart. Phys., 36, 183

Atoyan A. M., Dermer C. D., 2003, ApJ, 586, 79

Barwick S. W., 2007, J. Phys.: Conf. Ser., 60, 276

Becker J. K., 2008, Phys. Rep., 458, 173

Becker Tjus J., Eichmann B., Halzen F., Kheirandish A., Saba S. M., 2014, Phys. Rev. D, 89, 123005

Biermann P. L., Strittmatter P. A., 1987, ApJ, 322, 643

Celotti A., Ghisellini G., 2008, MNRAS, 385, 283

Chen D., 2008, in Caballero R., D'Olivo J. C., Medina-Tanco G., Nellen L., Sánchez F. A., Valdés-Galicia J. F., eds, Proc. Int. Cosmic Ray Conf., Vol. 4, Test of hadronic interaction models with data from the Pierre Auger Observatory, UNAM, Mexico City, Mexico, p. 103

Chiaberge M., Celotti A., Capetti A., Ghisellini G., 2000, A&A, 358, 104

Dermer C. D., 1995, ApJ, 446, L63

Dermer C. D., Menon G., 2009, High Energy Radiation from Black Holes: Gamma Rays, Cosmic Rays, and Neutrinos, Princeton Univ. Press, Princeton, NJ

Dermer C. D., Murase K., Inoue Y., 2014, J. High Energy Astrophys., 3, 29

Essey W., Kalashev O. E., Kusenko A., Beacom J. F., 2010, Phys. Rev. Lett., 104, 141102

Georganopoulos M., Kazanas D., 2003, ApJ, 594, L27

Ghisellini G., Tavecchio F., Chiaberge M., 2005, A&A, 432, 401

Ghisellini G., Maraschi L., Tavecchio F., 2009, MNRAS, 396, L105

Ghisellini G., Tavecchio F., Foschini L., Ghirlanda G., 2011, MNRAS, 414, 2674

Ghisellini G., Tavecchio F., Maraschi L, Celotti A., Sbarrato T., 2014, Nature, 515, 376

Giommi P., Padovani P., Polenta G., Turriziani S., D'Elia V., Piranomonte S., 2012, MNRAS, 420, 2899

Giommi P., Padovani P., Polenta G., 2013, MNRAS, 431, 1914

Giroletti M. et al., 2004, ApJ, 600, 127

Giroletti M., Giovannini G., Cotton W. D., Taylor G. B., Pérez-Torres M. A., Chiaberge M., Edwards P. G., 2008, A&A, 488, 905

Gorham P. W. et al., 2009, Astropart. Phys., 32, 10

Gorham P. W., Baginski F. E., Allison P., Liewer K. M., Miki C., Hill B., Varner G. S., 2011, Astropart. Phys., 35, 242

Kalashev O. E., Kusenko A., Essey W., 2013, Phys. Rev. Lett., 111, 041103

Kalashev O., Semikoz D., Tkachev I., 2015, J. Exp. Theor. Phys., 147, 3

Kimura S. S., Murase K., Toma K., 2014, preprint (arXiv:1411.3588)

Kotera K., Olinto A. V., 2011, ARA&A, 49, 119

Laha R., Beacom J. F., Dasgupta B., Horiuchi S., Murase K., 2013, Phys. Rev. D, 88, 043009

Loeb A., Waxman E., 2006, J. Cosmol. Astropart. Phys., 5, 003

McKinney J. C., 2006, MNRAS, 368, 1561

Mannheim K., 1995, Astropart. Phys., 3, 295

Meyer E. T., Fossati G., Georganopoulos M., Lister M. L., 2011, ApJ, 740, 98

Müller C. et al., 2014, A&A, 569, A115

Murase K., 2014, preprint (arXiv:1410.3680)

Murase K., Beacom J. F., 2013, J. Cosmol. Astropart. Phys., 2, 028

Murase K., Nagataki S., 2006, Phys. Rev. D, 73, 063002

Murase K., Dermer C. D., Takami H., Migliori G., 2012, ApJ, 749, 63

Murase K., Ahlers M., Lacki B. C., 2013, Phys. Rev. D, 88, 121301

Murase K., Inoue Y., Dermer C. D., 2014, Phys. Rev. D, 90, 023007

Nagai H. et al., 2014, ApJ, 785, 53

Nemmen R. S., Georganopoulos M., Guiriec S., Meyer E. T., Gehrels N., Sambruna R. M., 2012, Science, 338, 1445

Padovani P., Resconi E., 2014, MNRAS, 443, 474

Petropoulou M., Giannios D., Dimitrakoudis S., 2014, MNRAS, 445, 570

Piner B. G., Edwards P. G., 2004, ApJ, 600, 115

Piner B. G., Edwards P. G., 2014, ApJ, 797, 25

Piner B. G., Pant N., Edwards P. G., 2008, ApJ, 678, 64

Piner B. G., Pant N., Edwards P. G., 2010, ApJ, 723, 1150

Rieger F. M., Bosch-Ramon V., Duffy P., 2007, Ap&SS, 309, 119

Rossi P., Mignone A., Bodo G., Massaglia S., Ferrari A., 2008, A&A, 488, 795

Ruan J. J., Anderson S. F., Plotkin R. M., Brandt W. N., Burnett T. H., Myers A. D., Schneider D. P., 2014, ApJ, 797, 19

Sbarrato T., Ghisellini G., Maraschi L., Colpi M., 2012, MNRAS, 421, 1764

Sbarrato T., Padovani P., Ghisellini G., 2014, MNRAS, 445, 81

Tamborra I., Ando S., Murase K., 2014, J. Cosmol. Astropart. Phys., 9, 043

Tavecchio F., 2014, MNRAS, 438, 3255

Tavecchio F., Ghisellini G., 2008, MNRAS, 385, L98

Tavecchio F., Ghisellini G., 2014, MNRAS, 443, 1224

Tavecchio F., Ghisellini G., Ghirlanda G., Foschini L., Maraschi L., 2010, MNRAS, 401, 1570

Tavecchio F., Ghisellini G., Guetta D., 2014, ApJ, 793, L18 (Paper I)

Tchernin C., Aguilar J. A., Neronov A., Montaruli T., 2013, A&A, 555, A70

Urry C. M., Padovani P., 1995, PASP, 107, 803

Wang B., Zhao X., Li Z., 2014, J. Cosmol. Astropart. Phys., 11, 028

Waxman E., Bahcall J., 1997, Phys. Rev. Lett., 78, 2292

Waxman E., Bahcall J., 1999, Phys. Rev. D, 59, 023002

Yacobi L., Guetta D., Behar E., 2014, ApJ, 793, 48

Zandanel F., Tamborra I., Gabici S., Ando S., 2014, preprint (arXiv:1410.8697)

This paper has been typeset from a TEX/LATEX file prepared by the author.